Guo et al. *Zool. Res.* 2023, 44(1): 169−182
https://doi.org/10.24272/j.issn.2095-8137.2022.265

ZR | Zoological Research

Article Open Access

Unraveling the macroevolution of horseshoe bats (Chiroptera: Rhinolophidae: *Rhinolophus*)

Wei-Jian Guo[1,#], Yi Wu[1,#], Kai He[1], Yi-Bo Hu[2], Xiao-Yun Wang[1,*], Wen-Hua Yu[1,*]

[1] *Key Laboratory of Conservation and Application in Biodiversity of South China*, *School of Life Sciences*, *Guangzhou University*, *Guangzhou*, *Guangdong* 510000, *China*

[2] *CAS Key Laboratory of Animal Ecology and Conservation Biology*, *Institute of Zoology*, *Chinese Academy of Sciences*, *Beijing* 100101, *China*

ABSTRACT

Unraveling the diversification mechanisms of organisms is a fundamental and important macroevolutionary question regarding the diversity, ecological niche, and morphological divergence of life. However, many studies have only explored diversification mechanisms via isolated factors. Here, based on comparative phylogenetic analysis, we performed a macroevolutionary examination of horseshoe bats (Chiroptera: Rhinolophidae: *Rhinolophus*), to reveal the inter-relationships among diversification, intrinsic/extrinsic factors, and climatic ecological niche characteristics. Results showed a general slowing trajectory during diversification, with two dispersal events from Asia into Southeast Asia and Africa playing key roles in shaping regional heterogeneous diversity. Morphospace expansions of the investigated traits (e.g., body size, echolocation, and climate niche) revealed a decoupled pattern between diversification trajectory and trait divergence, suggesting that other factors (e.g., biotic interactions) potentially played a key role in recent diversification. Based on ancestral traits and pathway analyses, most *Rhinolophus* lineages belonging to the same region overlapped with each other geographically and were positively associated with the diversification rate, implying a competitive prelude to speciation. Overall, our study showed that multiple approaches need to be integrated to address diversification history. Rather than a single factor, the joint effects of multiple factors (biogeography, environmental drivers, and competition) are responsible for the current diversity patterns in horseshoe bats, and a corresponding multifaceted strategy is recommended to study these patterns in the future.

Keywords: Diversification; *Rhinolophus*; Historical biogeography; Abiotic/Biotic factors; Climatic niche characteristics; Competition

INTRODUCTION

Evolutionary biologists have long been concerned with the tremendous diversity of species, their phenotypes, and niches. Discovering the evolutionary explanations for such interspecific differences by identifying factors that influence biodiversity dynamics (increase or decrease in diversification rates) is a challenging task (Ezard et al., 2016). Traditionally,

Received: 10 October 2022; Accepted: 26 December 2022; Online: 28 December 2022

Foundation items: This study was supported by the National Natural Science Foundation of China (31970394, 32192421, 31300314) and Special Foundation for National Science and Technology Basic Research Program of China (2021FY100303)

[#]Authors contributed equally to this work

*Corresponding authors, E-mail: wangxy0607@163.com; wenhua_yu@gzhu.edu.cn

macroevolutionary progress has been thought to be driven either by intrinsic (biotic) or extrinsic (abiotic) factors, as evidenced by the Red Queen and Court Jester hypotheses, respectively. In the Red Queen hypothesis, evolution is considered a balance of biotic pressures, most notably competition. The strength of species competitiveness depends primarily on biotic factors, such as body size, interspecific interactions, local/regional ecological adaptations, and other life-history species-intrinsic traits that exist locally or over short time spans (Benton, 2009; Voje et al., 2015). In the Court Jester hypothesis (Barnosky, 2001), adaptation to stochastic environmental perturbations is considered the main driver of evolution and speciation. Species diversity results from historical abiotic factors, such as abrupt changes in climate, tectonic events, and explosive growth in food supply. Changes in abiotic factors provide new ecological opportunities for large-scale speciation regionally and globally over thousands and millions of years (Benton, 2009). Neither model has been proposed as exclusive (Benton, 2009; Condamine et al., 2018). Although additional studies have demonstrated that abiotic (paleoenvironmental) and biotic (species-intrinsic) drivers are equally important in regulating diversification (Ezard et al., 2016), these two factors are rarely studied simultaneously. The relative contributions of abiotic and biotic factors to diversity patterns can now be statistically assessed due to the wide availability of phylogenetic comparative methods that bridge phylogenies, species-intrinsic trait divergences, niche characteristics, historical climate fluctuations, and tectonic events (Alfaro et al., 2009; Rabosky, 2013; Rabosky et al., 2014a; Yu et al., 2012).

Horseshoe bats (*Rhinolophus* Lacépéde, 1799 (Chiroptera: Rhinolophidae Gray, 1825) are an ideal group for testing hypotheses on biotic (Red Queen) and abiotic (Court Jester) drivers of species richness. As the second largest bat genus, *Rhinolophus* currently includes more than 100 species (Csorba et al., 2003; Simmons, 2005; Wilson & Mittermeier, 2019). Horseshoe bats have evolved a high-duty-cycle (HDC) echolocation sonar system that enables them to detect flying insects in highly cluttered environments (Fenton, 1999; Jones & Teeling, 2006), which is believed to be adaptive for successful radiation (Jacobs & Bastian, 2018; Stoffberg et al., 2011), although some studies have found evidence of its constrained effect on subsequent evolution of diversity (Jacobs et al., 2013). Horseshoe bats are also notable for their heterogeneous species-intrinsic traits (e.g., body size and leaf-shaped nose) adapted to different habitats and environments, as well as their widespread distribution patterns throughout the Old World (Csorba et al., 2003; Simmons, 2005). Based on their previous phylogenetic framework (Stoffberg et al., 2010), Stoffberg et al. (2011) demonstrated a correlation between body size and echolocation, as predicted by the allometry hypothesis. However, subsequent studies based on this framework have included no more than 40 *Rhinolophus* species, accounting for less than 50% of the genus, or focused on speciation mechanisms only within certain *Rhinolophus* clades (e.g., Maluleke et al., 2017; Mutumi et al., 2017; Sun et al., 2013; Taylor et al., 2012).

In this study, we utilized multiple approaches to resolve the macroevolutionary progress of horseshoe bats. Using chronograms and phylogenetic comparative analyses, we explored the potential biotic traits that historically affected diversification and outlined the evolutionary progress traits. This study aimed to elucidate the inter-relationships among diversification, intrinsic/extrinsic factors, and climatic niche characteristics (Table 1).

MATERIALS AND METHODS

Phylogenetic inference and divergence time estimations

For phylogenetic analyses, we mined seven mitochondrial DNA (mtDNA) genes and 19 nucleotide DNA (nuDNA) genes (Supplementary Table S1) from 73 horseshoe bats and four *Hipposideros* bats from GenBank. Each gene was checked and edited using GENEIOUS v5.4 (Drummond et al., 2011) and aligned with MUSCLE (Edgar, 2004). All genes were concatenated into a supermatrix with a custom Python script. Each gene was specified as an independent partition for all subsequent phylogenetic analyses. The best-fit nucleotide substitution model for each locus was found using PartitionFinder v1.1.1 (Lanfear et al., 2012) based on Bayesian information criterion (BIC). The GTR+I+Γ model was determined as the best fit for most loci. A maximum-likelihood (ML) tree was inferred using RAxML v8.2 (Stamatakis, 2014), with phylogeny support assessed using 1 000 bootstrap replicates.

Divergence times were estimated using BEAST v1.8.2 (Suchard et al., 2018). Two separate analyses were run for 50 million generations under a birth-death process. After discarding the first five million generations as burn-in, two chain results were combined to render an estimated sample size (ESS)>200 (Drummond et al., 2006). Two calibrations were used with lognormal distribution priors (Foley et al., 2015; Meredith et al., 2011; Stoffberg et al., 2010; Teeling et al., 2005). The first calibration was set to 41 million years ago (Ma), with a lognormal standard deviation (*SD*) of 1 and a mean of 1 (95% prior credible interval (PCI)=41.12–44.14 Ma), yielding the putative age of Rhinolophidae and Hipposideridae divergence (Foley et al., 2015). The second calibration was set to 37 Ma, with a mean of 1 and *SD* of 1 (95% PCI=37.12–40.14 Ma), corresponding to the earliest possible emergence of horseshoe bats (McKenna & Bell, 1997; Simmons & Geisler, 1998). These priors are equivalent to previous analyses (Stoffberg et al., 2010).

Historical biogeographic analysis

To infer the broad-scale biogeographic history of extant horseshoe bats, likelihood-based geographic range reconstruction was conducted using RASP v3.2 (Yu et al., 2015). The distribution ranges of the horseshoe bats were categorized into six areas based on present separations of major landmasses (Csorba et al., 2003; Simmons, 2005) and the IUCN Red List of Threatened Species (International Union for Conservation of Nature, http://www.iucnredlist.org), i.e., Europe (E), Asia (A; except India and Southeast Asia), Africa (F), India (I), Southeast Asia (S), and Australia (U). Dispersal route availability models were developed based on geographic history and island chains, climatic data, and related ancestral area reconstruction (AAR) studies (Clayton et al., 2009; Foley

Table 1 Summary of diversification analyses (evolutionary models are divided by whether they are used to test hypotheses in favor of Red Queen or Court Jester. MCC, maximum clade credibility)

Type	Evolutionary model	Method used	Data used	Setting	Main results
Diversification pattern in temporal-scale and lineage-scale	Red Queen	Ape BAMM	MCC tree	Outline diversification dynamic	*Rhinolophus* has only one rate regime: slowed just prior to late Oligocene
Diversity-dependence	Red Queen	DDD (dd_ML) SEM	MCC tree + index of area overlap	Four models to test whether speciation declines with diversity and/or extinction increases with diversity	*Rhinolophus* has not reached carrying capacity but showed some degree of diversity dependence. Diversification is positively associated with competition
Bio-trait divergence pattern and diversification	Red Queen	QuaSSE BAMM SEM	100 posterior trees + MCC trees + trait data (forearm, echolocation, PCA 1~3 of climatic-niche)	Reconstruct ancestral state of bio-trait, test whether bio-trait, climatic-niche, or region impacted historical diversification, disentangle effects of these variables (area, diversity, range overlap) on diversification slowdowns	Diversification is not significantly associated with bio-traits, which subdivide niches/specialization
Environmental-driving diversification	Court Jester	RPANDA	100 posterior trees + MCC trees	Test whether diversification rates vary with paleoenvironment	Best fit by pure-birth linear speciation model with positive dependency on sea level across all posterior distributions for consensus phylogeny
Biogeographic history and pattern of distribution	Court Jester	RASP picante	MCC trees	Reconstruct ancestral area assumed chronogram and infer historical biogeographic event, analyze phylogenetic community structure	Asian (except India and Southeast Asia) origin, divided into two well-supported geographical clads. MPD and MNTD values of regions in Africa and Southeast Asia were significantly negative, suggesting phylogenetic clustering

et al., 2015; Morley, 2003; Scotese, 2001). All biogeographic analyses were performed on the maximum clade credibility (MCC) tree without outgroups using the Dispersal-Extinction-Cladogenesis model of range evolution in RASP. Three phases were delimited, and dispersal probabilities ranged from 0.01 for well-separated areas to 1.0 for contiguous landmasses. The maximum number of areas allowed in the reconstruction was set to two.

We also tested whether shifts in the diversification rate corresponded to nodes with transitions into unoccupied regions using the picante package (Kembel et al., 2010) in R environment v3.3.1 (R Core Team, 2018). Standardized effective sizes of the mean pairwise distance (MPD) and mean nearest taxon distance (MNTD) were calculated for each of the six biogeographic regions using the picante package. A null distribution of 1 000 simulated phylogenies was generated with randomly shuffled tips. Statistical significance was calculated by comparing the null distribution with our observed pattern.

Diversification analyses of Court Jester model

Paleodata with 11 variables included in the R package RPANDA (Morlon et al., 2016) were used for environment-dependent diversification models (Table 1). The 11 paleoenvironmental models, as well as constant-rate birth-death model, time-dependent speciation model (with and without constant extinction), and time-dependent extinction model (with constant speciation), were fitted to the MCC tree, with missing taxa accounted for by applying the relevant sampling fraction (Morlon et al., 2011). We tested speciation (λ) and extinction rates (μ) as constant, linear, and exponential functions of each paleoenvironmental model, as well as μ=0. The best-fit model for the tree was determined by Akaike information criterion (AIC), and corresponding speciation and extinction parameter estimates were recorded. Some variables (i.e., temperature ($\Delta^{18}O$) and land plant diversity) are directly biologically relevant to *Rhinolophus* clades, while other variables (i.e., CO_2, $\delta^{13}C$, coccolithophore diversity, foraminifera diversity, green algae diversity, Ostracoda diversity, Radiolaria diversity, sea level, and silica) are not directly biologically relevant to Rhinolophidae (Rebelo et al., 2010). In our analyses, variables that were not directly relevant were still included as negative controls.

Diversification analyses of Red Queen model

Diversification analyses across time and lineages: To detect and quantify heterogeneity in the evolutionary rates of the horseshoe bats, we focused on both temporal and lineage diversification variations using the R packages APE (Paradis et al., 2004) and BAMMtools (Rabosky et al., 2014b) with the MCC tree from BEAST analysis (Table 1).

To determine variations in temporal diversification, the reversible-jump MCMC approach implemented in BAMMtools v2.0 was also used to estimate diversification rates through time (Table 1). Appropriate speciation and extinction priors were chosen for each tree in the BAMMtools suite. The initial parameters and MCMC scaling operators and shift frequencies remained at default. The global sampling fraction parameter used to correct for incomplete sampling was set to 0.67 (73/109 sp). We assumed that rate changes occurred in 1 Ma increments. For analyses, 10 million generations (sampled every 1 000 generations) were run with four Markov chains and a temperature increment parameter of 0.1. The first 30% of generations were discarded as burn-in.

Diversity-dependent diversification analyses: As an initial burst of diversification followed by a slowdown to the present

was observed, diversity-dependent birth-death processes were modeled using the R package DDD (Etienne & Haegeman, 2012; Etienne et al., 2012) (Table 1). These processes emphasize that diversity is bounded or at equilibrium, meaning that diversity expands rapidly during early diversification and fills most niches, with saturation towards the present. Four different models were applied: (i) speciation linearly dependent on diversity without extinction (DDL), (ii) speciation exponentially dependent on diversity without extinction (DDX), (iii) speciation linearly dependent on diversity with extinction (DDL+E), and (iv) speciation exponentially dependent on diversity with extinction (DDX+E). For each model, the "missnumspec" option was set to the current number of described species minus the species used in this study. Models were run on the MCC tree from BEAST analysis, accounting for the number of incomplete taxon samplings.

Evolutionary progress of morphological, physiological, and climatic niche characteristics

Body size and echolocation are considered as two key traits in *Rhinolophus*, as the former is an adaptive trait affecting flight, roosting, reproduction, diet, and physiology of bats (Swartz et al., 2003), while the latter contributes to orientation and hunting, long regarded as under natural selection and constant divergence (Thomas et al., 2004; Willig, 2003). We chose forearm length (FA) to represent the body size dimension (Jacobs et al., 2013; Willig, 2003) and peak frequency (PF) recorded at rest to represent echolocation characteristics. The above data are reported in Csorba et al. (2003) and Wilson & Mittemeier (2019).

For climatic-niche traits, we downloaded the distribution ranges of each species from the IUCN Red List of Threatened Species. The 19 climatic variables derived from the WorldClim dataset (http://www.worldclim.org/) (30 s spatial resolution) (Hijmans et al., 2005) were extracted in ArcGIS (ESRI, 2011) for each species, and mean values were calculated for each variable for each species. To reduce the dimensionality of variables, principal component analysis (PCA) was performed on a matrix of 17 environmental variables (as BIO3 and BIO7 are linear combinations of other variables, they were excluded from analysis). The first three PCA scores (climatic-niche PC1, climatic-niche PC2, and climatic-niche PC3) accounted for more than 90% of total climate variation based on broken-stick distribution (Jackson, 1993) (Supplementary Figure S1) and were used for phylogenetic comparations. The scores were used to represent the climatic-niche characteristics of each horseshoe bat.

After log-transformation of FA and PF, the historical divergences of the five species-intrinsic candidates were modeled and visualized using BAMM and BAMMtools, respectively. Most prior specifications and Markov chain settings were the same as the analysis of diversification patterns. The models were run on the MCC tree (Table 1).

Estimating effects of morphological, physiological, climatic-niche characteristics, and species co-occurrence on diversification

To test whether the above quantitative traits affect horseshoe bat diversification, the phylogenetic likelihood-based quantitative state speciation and extinction (QuaSSE) method (Fitzjohn, 2010) was implemented using the Diversitree package in R (Fitzjohn, 2012) (Table 1). The consensus tree was trimmed by several species due to the lack of echolocation data. The speciation rate was modeled as both a constant and linear function of trait values, while extinction was implemented as a background process with an invariable rate (Fitzjohn, 2010). To verify the existence of a trait-diversification relationship, we also restrained the modeling of more complex functions of speciation and extinction (e.g., exponential drift rather than simple linear) because the process is time consuming and model parameterization is difficult (Fitzjohn, 2010).

To evaluate whether the co-occurrence of closely related species affects diversification, we examined spatial patterns within sympatric clades by obtaining the areas of species overlap, i.e., relative range overlap of clades (e.g., Machac et al., 2013; Wiens, 2011). Briefly, total habitat area of all species in the clade divided by geographic area of the clade was defined as the clade overlap index, ranging from 1 (all species in the clade show allopatric distribution, suggesting no geographic competition) to infinite (some species in the clade show sympatric distribution, suggesting possible increasing geographic competition). This is not a strict index of clade sympatry, as species may overlap at a macrogeographic scale but do not co-occur locally (e.g., low-elevation vs. high-elevation species). Nevertheless, it captures large-scale patterns of clade isolation and overlap that may influence the diversification of related species. All estimates mentioned above were calculated using a self-designed Python script with Hawth's Tools in ArcGIS v10.2.2. For other biotic traits (FA, PF, and climatic-niche PCs), the Brownian motion (BM) model and Ornstein-Uhlenbeck (OU) model of evolution were tested (Butler & King, 2004). Optimal models were selected separately based on AIC. Finally, the diversification rate for each horseshoe bat clade (i.e., each node of the phylogeny) was calculated using the "yule" function in the R package APE for subsequent path analyses.

To gain a comprehensive understanding of horseshoe bat evolution, we performed path analysis with structural equation modeling to disentangle the effects of candidate variables on diversification fluctuation (Table 1). Specifically, the diversification rates of species and biotic traits (i.e., FA, PF, climatic-niche PCs, and overlap index) for each node were used in path modeling to identify significant predictors decelerating the diversification of horseshoe bats (see Results). These analyses were conducted using Structural Equation Modeling (SEM) in the R environment (Fox, 2006).

Robustness test

To account for uncertainty in the topologies and branch times of our inferences, we conducted robustness tests not only to identify improved phylogenetic solutions for the dataset, but also to minimize false positives within our inferences. To achieve this, the top 100 likelihood score chronograms from the MCC tree were used as the "true tree". QuaSSE analysis, environment-dependent diversification models, and path analysis were replicated using the posterior tree, and parameter settings were the same as those for the MCC tree.

The validity of potential effort for species-intrinsic traits or paleoenvironmental fluctuations can be evaluated using the former two robustness tests, while the latter can shed light on the viability of the formulated causal model, for which trait and co-occurring species effects are independent variables with respect to the evolutionary history of horseshoe bats. We used custom Python scripts to ease the complexity and laboriousness of data mining and calculation. All analyses were conducted using R packages APE, geiger, RPANDA, Diversitree, and SEM.

RESULTS

Phylogeny and divergence time

Total combined data included 17 991 base pairs (bp) from seven mitochondrial genes and 19 nuclear genes (see Supplementary Table S1 for GenBank accession numbers), representing ~65% (73 horseshoe bats) of species and all major lineages within Rhinolophidae. Approximately 70% of the nodes were recovered with bootstrap support (BS) >80 (Supplementary Figure S2). Although deep phylogenetic relationships were not fully resolved (i.e., BS<80 for some nodes; Supplementary Figure S2), five of six subgenera (except *Ceolophyllus*) proposed by Csorba et al. (2003) were monophyletic and well supported by our ML phylogenies (subgenera are highlighted in colored boxes in Supplementary Figure S2). The ML phylogenies indicated that most weakly supported nodes were located within the radiations of the *Rhinophyllotis* clade (Csorba et al., 2003) (red circles in Supplementary Figure S2).

The relaxed Bayesian clock suggested that the most common ancestor of the horseshoe bats arose 37.6 Ma (95% highest posterior density (HPD) 37.02–38.72 Ma) (Figure 1A), a slightly younger estimation than proposed by Stoffberg et al. (2010). A rapid radiation trend based on a series of short branching events emerged during the late Eocene (Figure 1A). Similar to previous reports (Csorba et al., 2003; Stoffberg et al., 2010), two major *Rhinolophus* clades, namely the African and Oriental clades (Figure 1a), arose during the Oligocene, with ancestors of extant species present during the late Oligocene (African clade: 25.59 Ma, 95% HPD=19.96–31.00 Ma; Oriental clade: 32.13 Ma, 95% HPD=28.17–35.70 Ma; Figure 1A). Within the clades, diversification subsequently occurred during the late Oligocene and early Miocene (Figure 1A).

Biogeographic estimations

Optimal ancient area reconstructions (AARs) using the MCC chronogram required 26 dispersal events and 13 local extinction events to explain the current cross-continental distribution of horseshoe bats. The horseshoe bat crown-clade originated in Asia at the beginning of the late Eocene (Figure 2). The ancestor of the African and Oriental clades (37.6 Ma, 95% HPD 37.02–38.72 Ma) also originated in Asia, followed by independent dispersal events of African clade ancestors to Africa directly or via the European continent (Figure 2C). The phylogenetic community structure results (Africa: MPD.z=–7.693, *P*=0.001 and MNTD.z=–1.741, *P*=0.043; Table 2) indicated that dispersal events triggered subsequent radiations into the African region. Two early dispersal events contributed to extant Asian horseshoe bat prosperity, i.e., most common ancestors of *Aquias* (Csorba et al., 2003) and remaining oriental members from Asia to Southeast Asia in the late Oligocene (Figure 2A). Regional radiation was also supported by our phylogenetic community structure analyses (Southeast Asia: MPD.z=–9.354, *P*=0.001 and MNTD.z=–2.583, *P*=0.005; Table 2). Interestingly, the AAR results also highlighted redispersal events from Southeast Asia to Asia in shaping the current wide distribution range of some Oriental species (e.g., *Rhinolophus pearsoni* Horsfield, 1851 and *Rhinolophus affinis* Horsfield, 1823) (Figure 2C).

Macroevolutionary dynamics

The diversification analysis results are presented in Table 1.

Diversification in Red Queen model

Based on lineages-through-time (LTT) plots, a declining trend in *Rhinolophus* diversification from the Eocene to the present was observed (Figure 1B). The BAMM model revealed a globally declining trend of diversification (posterior probability of one regime=0.73 vs. posterior probability of two regimes (one global declining regime and uncertain regimes/clades=0.22) and indicated that no particular lineage/clade underwent exceptional diversification. The best-fit DDD model (extinction rate of 0 and carrying capacity of 202 species (ΔAICc>2; Table 3) supported a diversity-dependent process with decreasing speciation, consistent with the BAMM results.

The rate of FA divergence moderately increased toward the present, supporting an accelerated differentiation process. Similar patterns and non-specific regimes also emerged in modeling of climatic-niches PC2 and PC3 (Figure 3D, E). In contrast, the divergence rate of PF varied markedly at the clade and temporal scales. The posterior probabilities of two and three regimes from PF were comparable, and their divergence trends revealed fluctuations in trait differentiation from the late Miocene to the present (Figure 3B). The QuaSSE results indicated that the minimal models were most favored when analyzing FA, PF, and climatic-niche PC1, PC2, and PC3 scores, and implied that none of the candidates influenced historical diversification (Table 4). Results based on the 100 highest likelihood trees showed consistent results with the MCC tree, while the effect of PC1 on diversification also emerged in the diversification dynamics (Supplementary Figure S3).

Path analyses were conducted to describe directed dependencies among a set of variables, including FA, PF, climatic-niche PCs, clade overlap index, and diversification. Only the clade overlap index (total effects=0.50, *P*<0.001) showed a direct effect on historical diversification progress (Figure 4), with no other factor showing a significant relationship with diversification. To overcome uncertainty bias in the horseshoe bat relationship, path analyses were replicated based on the 100 best trees. However, only 30% of trees indicated that the clade overlap index (competition) was associated with diversification (Table 5). Except for shifts in echolocation frequency and climate niche PC1, all other factors showed significant effects on horseshoe bat

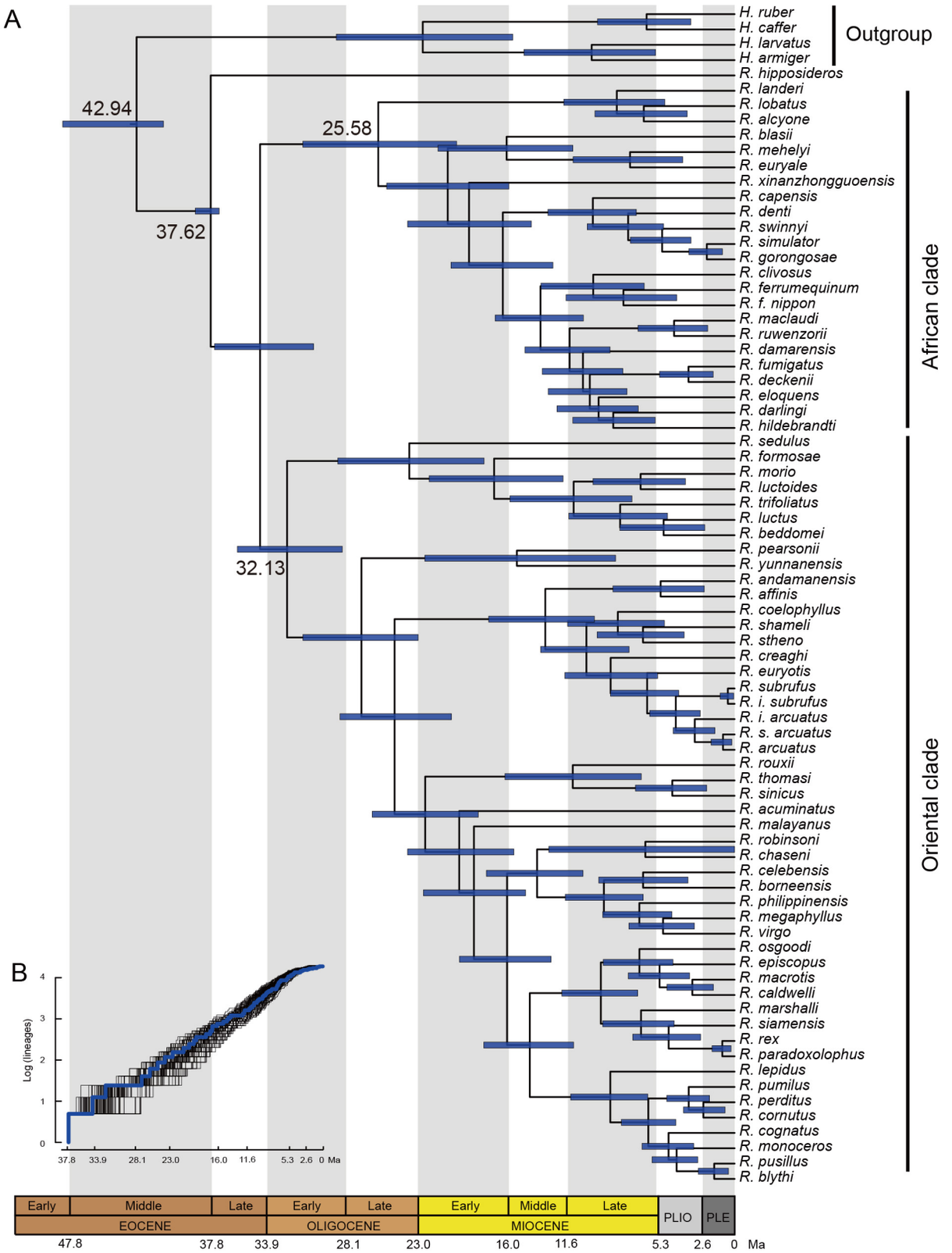

Figure 1 Divergence times of *Rhinolophus*

A: Time-calibrated phylogenetic tree of *Rhinolophus* derived from BEAST. For each node, estimated time of divergence is indicated with a bar representing 95% HPD intervals of node ages. B: Lineage-through-time plot, with gray lines representing LTT plots for a set of 100 PP trees.

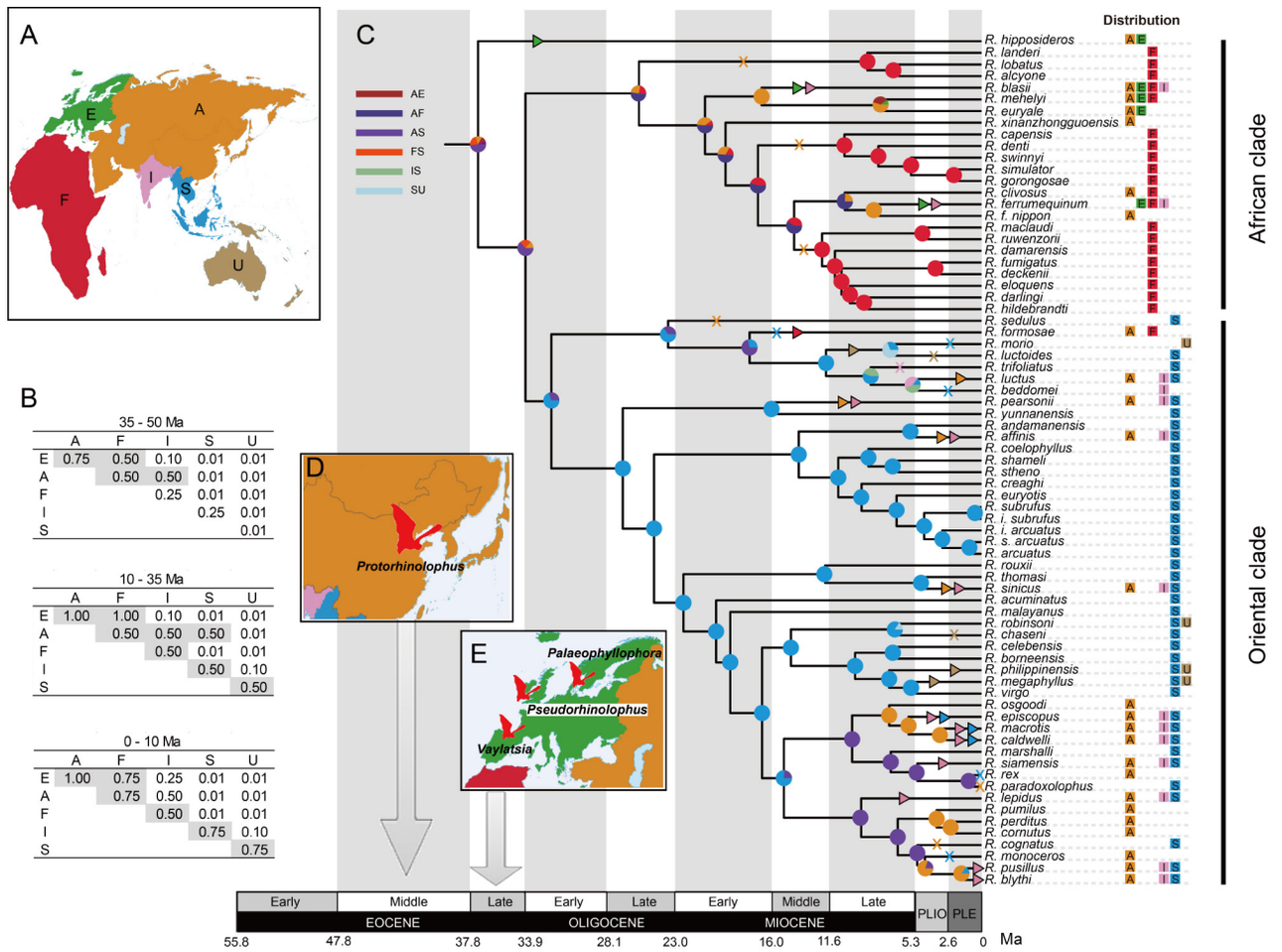

Figure 2 Ancestral area reconstruction for *Rhinolophus*

A: Areas assigned to horseshoe bats in this study. E, Europe; A, Asia (except India and Southeast Asia); F, Africa; I, India; S, Southeast Asia; U, Australia. B: Probabilities of relative dispersal among six areas as a box matrix on left side of graph (0.01, none; 0.1, low; 0.25, medium-low; 0.5, medium; 0.75, medium-high; 1, high). C: Ancestral area reconstructions of *Rhinolophus*. Range expansion and local extinction are indicated by "triangle" and "X" on chronogram branches, respectively. D, E: Discovery place of horseshoe bat fossils.

Table 2 Standardized effective size of mean pairwise distance (MPD.z) and mean nearest taxon distance (MNTD.z) for *Rhinolophus* communities in six biogeographic regions

Regime	ntaxa	MPD.z	*P*	MNTD.z	*P*
Europe	5	–0.670	0.196	–0.345	0.369
Asia (except India and Southeast Asia)	25	–1.693	0.060	–0.061	0.461
Africa	**21**	**–7.693**	**0.001**	**–1.741**	**0.043**
India	14	–1.542	0.079	–0.994	0.158
Southeast Asia	**40**	**–9.354**	**0.001**	**–2.583**	**0.005**
Australia	4	–1.459	0.092	–1.212	0.119

Significant values are in bold.

diversification based on robustness tests (Table 5), suggesting that these factors may establish an intricate relationship web within the evolutionary process.

Diversification in Court Jester model

AAR analysis suggested that extant horseshoe bats originated in Asia (except for India and Southeast Asia) (Figure 2C), in agreement with new fossils from the middle Eocene of Shanghuang (Jiangsu Province, China) (Ravel et al., 2014). Most species, however, were concentrated in Southeast Asia and Africa, rather than their provenance region (Figure 2C). The MPD and MNTD values for the Southeast Asian and African regions were significantly negative, suggesting phylogenetic clustering (Table 2). These results highlight the important role of tectonic movement and dispersal events in historical diversification, suggesting that the Court Jester model may play a role in diversification trajectories.

Table 3 Results from diversity-dependence diversification analyses in DDD for horseshoe bats

Models	NP	log L	AICc	ΔAIC	λ	μ	K
DDL	**2**	**−240.588**	**485.348**	**0**	**0.152**	**–**	**202.333**
DDX	2	−242.064	488.300	2.952	0.200	$9.043e^{-4}$	Inf
DDL+E	3	−240.606	487.560	2.152	0.156	$3.058e^{-4}$	196.482
DDX+E	3	−242.076	490.500	5.152	0.201	$5.958e^{-4}$	Inf

Model with highest support (lowest AICc) is shown in bold; this model received significant support (ΔAIC>2), although models including extinction were best supported. NP, number of parameters; log L, log-likelihood; AICc, corrected Akaike Information Criterion; ΔAICc, difference in AICc between model with lowest AICc and others. Parameter estimates: λ, speciation rate; μ, extinction rate; K, estimated "carrying capacity" (i.e., ecological limits) for which "Inf" means that carrying capacity is infinite.

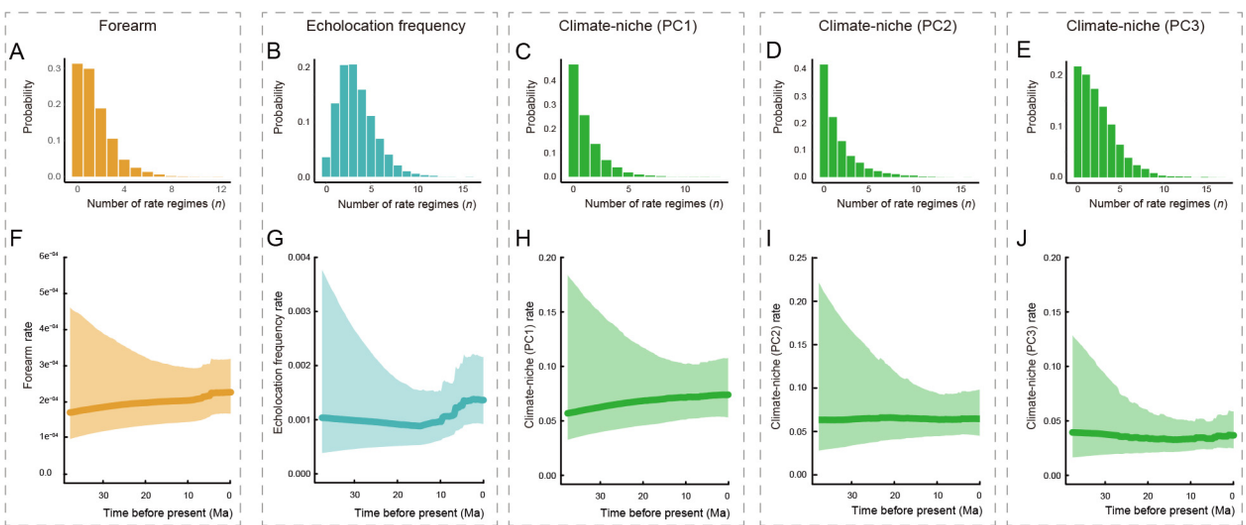

Figure 3 Rate through time and posterior probabilities of the number of rate regimes present in the horseshoe bat dataset for forearm (A, F), echolocation frequency (B, G), climatic-niche (PC1) (C, H), climatic-niche (PC2) (D, I), and climatic-niche (PC3) (E, J)

Shaded area represents 10%–90% credible region of the distribution of rates through time.

Based on the MCC tree, the overall diversification trend without dramatic fluctuations implied no turnover within the horseshoe bat macroevolutionary trajectory. This conclusion was supported by the ML-based paleoenvironment-dependent pure-birth linear speciation model, which was positively related to past sea level, an unpredicted abiotic factor (Table 6). Furthermore, analyses of environment-dependent factors using 100 posterior trees with the highest likelihood scores revealed that ~40% of trees favored sea-level change in modeling, while ~15% favored green algae diversity. Although none of the abiotic candidates in RPANDA were suitable for modeling horseshoe bat diversification, these data may provide new insight in future studies and may involve confounding variables.

DISCUSSION

Divergence times and historical biogeography of horseshoe bats

Most previous studies broadly agree with our molecular phylogeny, including monophyly of Rhinolophidae, African clade, and Oriental clade (Guillén-Servent et al., 2003; Stoffberg et al., 2010, Figure 2C). Compared to the rapid diversification in the early phase of Rhinolophidae in the late Eocene, our chronograms revealed a lack of branching events in the middle Eocene after the split with Hipposideridae approximately 43 Ma, a slightly older estimate than previously predicted using high-level representations (Álvarez-Carretero et al., 2022; Eick et al., 2005; Foley et al., 2015; Shi & Rabosky, 2015; Stoffberg et al., 2010). The estimated age of the most recent common ancestor of extant Rhinolophidae (37.6 Ma) overlaps the estimate of Stoffberg et al. (2010) and is congruent with early Rhinolophidae fossils from the middle Eocene, such as *Protorhinolophus* Ravel, 2013 in Asia and *Vaylatsia* Sige, 1990 in Europe (Eiting & Gunnell, 2009; Gunnell & Simmons, 2005; Ravel et al., 2014; Simmons & Geisler, 1998). Our AAR model indicated an Asian provenance for extant horseshoe bats, broadly consistent with previous inferences (Stoffberg et al., 2010; Yu et al., 2014). This result is also congruent with the oldest known fossil of Rhinolophidae, *Protorhinolophus shanghuangensis*, recently found in the middle Eocene Shanghuang (China) fissure fillings in Asia (Ravel et al., 2014). After originating in Asia, two dispersal events into Africa and Southeast Asia during the Miocene played key roles in forming present-day fauna (Figure 2C). Phylogenetic community structure (MPD.z and MNTD.z scores) analyses of each region indicated that the co-occurrence of taxa from Africa and Southeast Asia was more closely related than expected from the null distribution, which could be interpreted as either regional explosive radiation

Table 4 Model-fitting results for trait-dependent diversification models (QuaSSE)

	Df	ln *L*	AIC	ChiSq	Pr (>|Chi|)
FA					
Minimal	**3**	**–116.093**	**238.186**	**N/A**	**N/A**
Linear	4	–115.750	239.500	0.687	0.407
Sigmoidal	6	–115.758	243.517	0.670	0.880
Hump	6	–115.569	243.139	1.048	0.790
Echo					
Minimal	**3**	**–164.109**	**334.218**	**N/A**	**N/A**
Linear	4	–164.095	336.191	0.027	0.870
Sigmoidal	6	–163.833	339.666	0.552	0.907
Hump	6	–163.896	339.791	0.426	0.935
Bio_PC1					
Minimal	**3**	**–279.553**	**565.107**	**N/A**	**N/A**
Linear	4	–278.184	564.368	2.738	0.098
Sigmoidal	6	–276.747	565.495	5.612	0.132
Hump	6	–277.164	566.329	4.778	0.189
Bio_PC2					
Minimal	**3**	**–278.810**	**563.620**	**N/A**	**N/A**
Linear	4	–278.805	565.670	0.011	0.917
Sigmoidal	6	–277.422	566.844	2.776	0.427
Hump	6	–276.764	565.527	4.093	0.252
Bio_PC3					
Minimal	**3**	**–269.731**	**545.461**	**N/A**	**N/A**
Linear	4	–269.502	547.004	0.457	0.499
Sigmoidal	6	–268.940	549.880	1.582	0.664
Hump	6	–268.754	549.509	1.953	0.582

Optimal models are in bold. Df, degrees of freedom; ln *L*, log likelihood; AIC, Akaike information criterion; ChiSq, *chi*-square test value; Pr (>|Chi|), probability value for *chi*-square value. N/A: Not available.

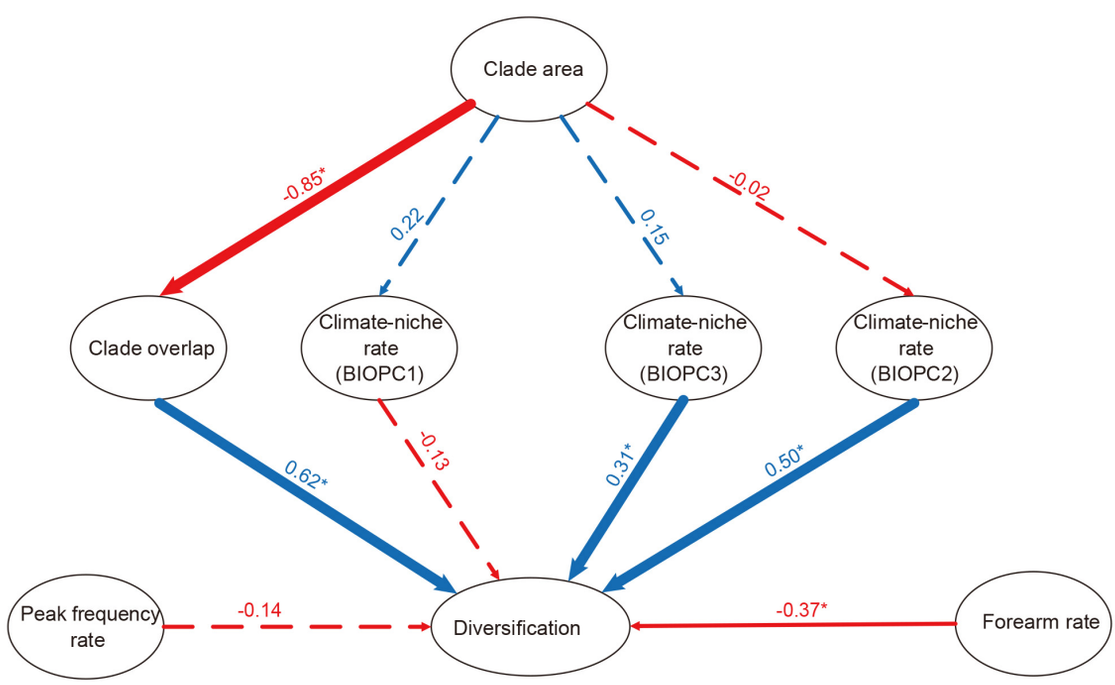

Figure 4 Plot of path analyses

Solid line shows significant relationship, while dashed line shows no significant relationship. Standardized correlation coefficients are shown above arrows connecting variables. Statistically significant correlation coefficients (P<0.05) are marked with an asterisk.

Table 5 Robustness tests in pathway analysis

	Number of significant results	Mean of significant total effects	*SD* of significant total effects	Number of non-significant results	Mean of non-significant total effects	*SD* of non-significant total effects
Rate of forearm → divergence rate	51	0.90	1.26	49	0.04	0.14
Rate of echolocation frequency → divergence rate	35	–1.08	1.41	65	–0.07	0.12
Rate of climatic-niche PC1 → divergence rate	47	–1.10	0.94	53	–0.09	0.12
Rate of climatic-niche PC2 → divergence rate	50	0.52	0.94	50	–0.08	0.12
Rate of climatic-niche PC3 → divergence rate	59	0.29	0.90	41	0.15	0.09
Overlap index → divergence rate	32	0.30	0.38	68	–0.07	0.15

Table 6 Best model of environment-dependent analysis

Model name	Explanation	Speciation rate [1]	Speciation rate [2]	Extinction rate [1]	Extinction rate [2]	LH	AICc	Robustness
sea level_l	**Sea-level linear functions birth-death model (without extinction)**	**0.131**	**0.003**	**N/A**	**N/A**	**–237.631**	**479.434**	**42**
greenalgae_l	Green algae diversity linear functions birth-death model (without extinction)	0.073	0.006	N/A	N/A	–239.035	482.242	9
coccolithophore_l	Coccolithophore diversity linear functions birth-death model (without extinction)	0.162	–0.006	N/A	N/A	–239.437	483.045	8
InfTemp_l	Temperature linear functions birth-death model (without extinction)	0.041	0.013	N/A	N/A	–239.915	484.001	2
greenalgae_exp	Green algae diversity exponential functions birth-death model (without extinction)	0.096	0.041	N/A	N/A	–240.097	484.366	15
radiolaria_l	Radiolaria diversity linear functions birth-death model (without extinction)	0.155	–0.008	N/A	N/A	–240.250	484.671	1
ostracoda_l	Ostracoda diversity linear functions birth-death model (without extinction)	–0.240	0.009	N/A	N/A	–240.785	485.742	1
bd_c_noext	Constant-rate birth–death model (without extinction)	0.109	N/A	N/A	N/A	–242.011	486.079	8
InfTemp_c	Temperature constant functions birth-death model (without extinction)	0.109	N/A	N/A	N/A	–242.011	486.079	0
co2_c	CO_2 constant functions birth-death model (without extinction)	0.109	N/A	N/A	N/A	–242.011	486.079	0
d13c_c	$\delta^{13}C$ constant functions birth-death model (without extinction)	0.109	N/A	N/A	N/A	–242.011	486.079	0
coccolithophore_c	Coccolithophore diversity constant functions birth-death model (without extinction)	0.109	N/A	N/A	N/A	–242.011	486.079	0
foraminifera_c	Foraminifera diversity constant functions birth-death model (without extinction)	0.109	N/A	N/A	N/A	–242.011	486.079	0
greenalgae_c	Green algae diversity constant functions birth-death model (without extinction)	0.109	N/A	N/A	N/A	–242.011	486.079	0
landplant_c	Land plant diversity constant functions birth-death model (without extinction)	0.109	N/A	N/A	N/A	–242.011	486.079	0
ostracoda_c	Ostracoda diversity constant functions birth-death model (without extinction)	0.109	N/A	N/A	N/A	–242.011	486.079	0
radiolaria_c	Radiolaria diversity constant functions birth-death model (without extinction)	0.109	N/A	N/A	N/A	–242.011	486.079	0
sea level_c	Sea-level constant functions birth-death model (without extinction)	0.109	N/A	N/A	N/A	–242.011	486.079	0
silica_c	Silica constant functions birth-death model (without extinction)	0.109	N/A	N/A	N/A	–242.011	486.079	0
ostracoda_exp	Ostracoda diversity exponential functions birth-death model (without extinction)	0.038	0.027	N/A	N/A	–241.647	487.466	0
landplant_l	Fits land plant diversity linear functions birth-death model (without extinction)	0.119	0.000	N/A	N/A	–241.682	487.535	1
foraminifera_l	Foraminifera diversity linear functions birth-death model (without extinction)	0.000	0.002	N/A	N/A	–241.731	487.633	0
bd_l_noext	Time-dependent speciation linear model (without extinction)	0.097	0.001	N/A	N/A	–241.753	487.677	0
sea level_exp	Sea-level exponential functions birth-death model (without extinction)	0.108	0.001	N/A	N/A	–241.805	487.781	0
foraminifera_exp	Foraminifera diversity exponential functions birth-death model (without extinction)	0.055	0.013	N/A	N/A	–241.808	487.788	0

Continued

Model name	Explanation	Speciation rate [1]	Speciation rate [2]	Extinction rate [1]	Extinction rate [2]	LH	AICc	Robustness
co2_exp	CO_2 exponential functions birth-death model (without extinction)	4.975	–3.897	N/A	N/A	–241.811	487.794	0
bd_exp_noext	Time-dependent speciation exponential model (without extinction)	0.101	0.008	N/A	N/A	–241.816	487.804	0
InfTemp_exp	Temperature exponential functions birth-death model (without extinction)	0.101	0.009	N/A	N/A	–241.863	487.896	0
silica_exp	Silica exponential functions birth-death model (without extinction)	0.167	–0.608	N/A	N/A	–241.881	487.934	0
landplant_exp	Land plant diversity exponential functions birth-death model (without extinction)	0.115	–0.002	N/A	N/A	–241.887	487.946	0
coccolithophore_exp	Coccolithophore diversity exponential functions birth-death model (without extinction)	0.119	–0.005	N/A	N/A	–241.892	487.955	0
silica_l	Silica linear functions birth-death model (without extinction)	0.129	–0.030	N/A	N/A	–241.959	488.090	0
radiolaria_exp	Radiolaria diversity exponential functions birth-death model (without extinction)	0.114	–0.004	N/A	N/A	–241.963	488.097	1
d13c_l	$\delta^{13}C$ linear functions birth-death model (without extinction)	0.083	0.011	N/A	N/A	–241.964	488.099	4
d13c_exp	$\delta^{13}C$ exponential functions birth-death model (without extinction)	0.060	0.240	N/A	N/A	–241.972	488.116	0
co2_l	CO_2 linear functions birth-death model (without extinction)	0.136	–0.026	N/A	N/A	–241.978	488.127	5
bd_c	Constant-rate birth–death model	0.109	N/A	0.000	N/A	–242.011	488.194	0
bd_l	Time-dependent speciation linear model (with extinction)	0.097	0.001	0.000	N/A	–241.753	489.853	0
bd_exp	Time-dependent speciation exponential model (with extinction)	0.101	0.008	0.000	N/A	–241.816	489.980	0
bd_ext_l	Time-dependent extinction linear model (with constant speciation)	0.110	N/A	0.002	0.000	–242.007	490.362	0
bd_ext_exp	Time-dependent extinction exponential model (with constant speciation)	0.109	N/A	0.000	-0.026	–242.013	490.373	0

Model with highest support (lowest AICc) is shown in bold. For each model, corresponding speciation/extinction rates ranged from [1] to [2]. N/A: Not available.

(Mazel et al., 2016) or phylogenetic niche conservatism (Losos, 2008). However, the former may be more plausible given the subsequent radiation of colonization from Asia and gradual joining of continents. In addition, the arrival of Rhinolophidae in western Europe may have been a stepping-stone of the dispersal route from Asia into Africa, which is not explicitly indicated by our AAR results (Figure 2C), or a separate dispersal from their ancestors (e.g., *Rhinolophus hipposideros* Bechstein, 1800 in Figure 2C) (Ravel et al., 2014), which needs further study.

Decelerating diversification of horseshoe bats

Characterizing diversification dynamics (i.e., how and when net diversification varies across time, space, and clades) is a prerequisite for understanding the historical determinants of biodiversity dynamics and exploring the complex interactions between diversification and biotic traits (Moen & Morlon, 2014). The biological causes of slowdown are multifarious and complex. By integrating paleoenvironmental changes, distribution areas, species-intrinsic traits, climatic-niche characteristics, species overlap, and chronograms, our results showed that species within each clade tended to occur in nearby geographic areas and emphasized the significant role of niche divergence and competition (clade overlap index) among related species in the historical cladogenesis of horseshoe bats (Figure 4). Under the framework of niche differentiation (tropical and temperate zones), this pattern belongs to diversity-dependent diversification (best model: speciation is linearly dependent on diversity with extinction, carrying capacity of 202 species, Table 3), which also corresponds to radiation.

Macroevolution of horseshoe bats via Red Queen and Court Jester

Based on chronogram visualization of diversification trajectories and short branding patterns, our results suggested that although the horseshoe bats experienced radiation in the early phase, synchrony of interspecific diversification and divergence of HDC call frequency did not emerge (Figure 3; Supplementary Figure S4). HDC is a striking bio-trait in horseshoe bats, allowing echolocation at higher frequencies than bats from other families with similar body size ranges, such as Molossidae Castelnau, 1855 and Vespertilionidae Gray, 1821 (Jones, 1999). HDC is hypothesized to have arisen as an adaptation to cluttered habitats, thereby permitting specialization (Jacobs & Bastian, 2018; Jones & Holderied, 2007; Jones & Teeling, 2006; Stoffberg et al., 2011). It may also have allowed their ancestors to colonize new cluttered habitats, leading to ecological release by relaxing natural selection acting on one or more ecological traits (Yoder et al., 2010). However, rapid speciation in this phase was not characterized by synchrony among our candidates, including body size, climatic-niche characteristics, and main echolocation frequency. Coincidently, conservatism

in body size from fossil records in the Eocene (Eiting & Gunnell, 2009; Ravel et al., 2014) supports such synchrony. The widespread distribution patterns from Eocene fossil records and frequent dispersals from our AAR results highlight the importance of biogeographic events in diversification (Figure 2). Under such an assumption, conservatism in our candidates in the early stage may be justified, as no apparent natural selection triggering fast trait variation can be found, at least for the candidates herein, due to the abundance of exploitable resources, niches, and ecological opportunities. Phenotypic and niche conservatism may be derived from stagnation in resource partitioning during this phase. Support of monophyly for the presumed subgenera in our phylogenies suggests early divergence in the leaf nose structure, implying that exploration of these structures could offer a way to solve the puzzle of early rhinolophid radiation.

Another striking finding of our study concerns the relationship between the change rate of the five species-intrinsic candidates, overlap index, and diversification when using structural equation modeling. Path analysis only corroborated the significant effects of the overlap ratio. The strongest link between the diversification rate and overlap ratio (MCC tree: total effects=0.50, P<0.001; 32% of posterior probability trees; Table 5, Figure 4) belonged to diversity-dependent diversification, thus emphasizing increasingly rigorous competition among closely related species for limited resources or niches, ultimately affecting speciation and extinction dynamics (Moen & Morlon, 2014; Rabosky, 2013; Weir & Mursleen, 2013). Although the robustness tests indicated that FA, climatic-niche PC2, and climatic-niche PC3 had potential effects on diversification, these effects were not detected in the MCC tree-based SEM models, further implying progress in ecological diversification via competition-mediated diversification. Interpretations of the tests are somewhat unclear because, on the one hand, the meaning of each PC is ambiguous due to the nature of dimensionality reduction; on the other hand, the estimated diversification rate reflected the divergence rate of each node along our chronograms. Furthermore, the factors responsible for horseshoe bat diversification remained undefined in the pathway analysis within the robustness test, possibly due to the uncertainty of phylogeny and branching time. Thus, more detailed analyses of the historical diversification processes underlying changes in factors are required.

Based on the potential effects of the sigma of climatic-niche PC2 and PC3 scores on the divergence rate, ecological diversification in Rhinolophidae was expected to accompany speciation (Figure 4, Table 5). Here, PC3 was weighted exclusively by precipitation of the warmest quarter (BIO18, Supplementary Figure S1), while PC2 was weighted by precipitation seasonality. The positive relationship between plant diversity and precipitation of the warmest quarter in tropical regions (Gwitira et al., 2014) suggests that the change rate in Rhinolophidae diversification may be linked to local niche heterogeneity and increased tropical plant diversity due to the concentration of horseshoe bats in the region during the Tertiary period. This progression fits into the conceptual framework of character displacement (Brown & Wilson, 1956), a long-term mechanism for enabling closely related species to overlap/coexist (Pfennig & Pfennig, 2009). Under this scenario, diversification and divergence in other species-intrinsic traits would lead to niche evolution in horseshoe bats, possibly reducing resource competition and reproductive interactions between species.

Interestingly, unlike recent studies highlighting the effects of paleoenvironmental fluctuations and tectonic events on macroevolution (Meredith et al., 2011; Steeman et al., 2009; Yu et al., 2014), only one Court Jester factor (sea level) herein revealed significant effects on historical diversification fluctuations (Table 6). Although, sea-level fluctuations have been shown to promote plant diversification (Guo et al., 2015), which may indirectly affect horseshoe bat food or habitat, we still argue that such results may arise from weak methodological power during detection or lack of well-designed analyses, which may shed light on the complex causal interactions among diversification, abiotic factors, and trait divergence. Furthermore, the radiation of the African and Oriental clades suggested by our phylogenetic community structure (Table 2) explicitly supported the strong roles of dispersal events and tectonic events, including plate collisions among the Asian, African, and Southeast Asian continents, and island building and growth, especially in Southeast Asia. However, further research should be conducted to elucidate the influence of Court Jester factors on horseshoe bat diversification.

SUPPLEMENTARY DATA

Supplementary data to this article can be found online.

COMPETING INTERESTS

The authors declare that they have no competing interests.

AUTHORS' CONTRIBUTIONS

W.H.Y. and Y.W. designed the study. W.J.G., X.Y.W., W.Y., K.H., Y.B.H., and W.H.Y. performed the data analyses. W.H.Y., X.Y.W., and W.J.G. wrote the manuscript. X.Y.W., W.H.Y., and W.J.G. revised the manuscript. All authors read and approved the final version of the manuscript.

REFERENCES

Alfaro ME, Santini F, Brock C, Alamillo H, Dornburg A, Rabosky DL, et al. 2009. Nine exceptional radiations plus high turnover explain species diversity in jawed vertebrates. *Proceedings of the National Academy of Sciences of the United States of America*, **106**(32): 13410−13414.

Álvarez-Carretero S, Tamuri AU, Battini M, Nascimento FF, Carlisle E, Asher RJ, et al. 2022. A species-level timeline of mammal evolution integrating phylogenomic data. *Nature*, **602**(7896): 263−267.

Barnosky AD. 2001. Distinguishing the effects of the Red queen and Court Jester on Miocene mammal evolution in the northern Rocky Mountains. *Journal of Vertebrate Paleontology*, **21**(1): 172−185.

Benton MJ. 2009. The Red Queen and the Court Jester: species diversity and the role of biotic and abiotic factors through time. *Science*, **323**(5915): 728−732.

Brown WL, Wilson EO. 1956. Character displacement. *Systematic Zoology*, **5**(2): 49−64.

Butler MA, King AA. 2004. Phylogenetic comparative analysis: a modeling approach for adaptive evolution. *The American Naturalist*, **164**(6): 683−695.
Clayton JW, Soltis PS, Soltis DE. 2009. Recent long-distance dispersal overshadows ancient biogeographical patterns in a pantropical Angiosperm family (Simaroubaceae, Sapindales). *Systematic Biology*, **58**(4): 395−410.
Condamine FL, Rolland J, Höhna S, Sperling FAH, Sanmartín I. 2018. Testing the role of the Red Queen and Court Jester as drivers of the macroevolution of Apollo butterflies. *Systematic Biology*, **67**(6): 940−964.
Csorba G, Ujhelyi P, Thomas N. 2003. Horseshoe Bats of the World (Chiroptera: Rhinolophidae). Shropshire: Pelagic Publishing Press.
Drummond AJ, Ashton B, Buxton S, Cheung M, Cooper A, Duran C, et al. 2011. Geneious v5.4. http://www.geneious.com.
Drummond AJ, Ho SYW, Phillips MJ, Rambaut A. 2006. Relaxed phylogenetics and dating with confidence. *PLoS Biology*, **4**(5): e88.
Edgar RC. 2004. MUSCLE: multiple sequence alignment with high accuracy and high throughput. *Nucleic Acids Research*, **32**(5): 1792−1797.
Eick GN, Jacobs DS, Matthee CA. 2005. A nuclear DNA phylogenetic perspective on the evolution of echolocation and historical biogeography of extant bats (Chiroptera). *Molecular Biology and Evolution*, **22**(9): 1869−1886.
Eiting TP, Gunnell GF. 2009. Global completeness of the bat fossil record. *Journal of Mammalian Evolution*, **16**(3): 151−173.
ESRI. 2011. ArcGIS desktop: release 10. Redlands: Environmental Systems Research Institute.
Etienne RS, Haegeman B. 2012. A conceptual and statistical framework for adaptive radiations with a key role for diversity dependence. *The American Naturalist*, **180**(4): E75−E89.
Etienne RS, Haegeman B, Stadler T, Aze T, Pearson PN, Purvis A, et al. 2012. Diversity-dependence brings molecular phylogenies closer to agreement with the fossil record. *Proceedings of the Royal Society B:Biological Sciences*, **279**(1732): 1300−1309.
Ezard THG, Quental TB, Benton MJ. 2016. The challenges to inferring the regulators of biodiversity in deep time. *Philosophical Transactions of the Royal Society B:Biological Sciences*, **371**(1691): 20150216.
Fenton MB. 1999. Describing the echolocation calls and behaviour of bats. *Acta Chiropterologica*, **1**(2): 127−136.
Fitzjohn RG. 2010. Quantitative traits and diversification. *Systematic Biology*, **59**(6): 619−633.
Fitzjohn RG. 2012. Diversitree: comparative phylogenetic analyses of diversification in R. *Methods in Ecology and Evolution*, **3**(6): 1084−1092.
Foley NM, Thong VD, Soisook P, Goodman SM, Armstrong KN, Jacobs DS, et al. 2015. How and why overcome the impediments to resolution: lessons from rhinolophid and hipposiderid bats. *Molecular Biology and Evolution*, **32**(2): 313−333.
Fox J. 2006. Teacher's corner: structural equation modeling with the sem package in R. *Structural Equation Modeling:A Multidisciplinary Journal*, **13**(3): 465−486.
Guillén-Servent A, Francis CM, Ricklefs RE. 2003. Phylogeny and biogeography of the horseshoe bats. *In*: Csorba G, Ujhelyi P, Thomas N. Horseshoe Bats of the World (Chiroptera: Rhinolophidae). Shropshire: Alana Books.
Gunnell GF, Simmons NB. 2005. Fossil evidence and the origin of bats. *Journal of Mammalian Evolution*, **12**(1): 209−246.
Guo YY, Luo YB, Liu ZJ, Wang XQ. 2015. Reticulate evolution and sea-level fluctuations together drove species diversification of slipper orchids (*Paphiopedilum*) in South-East Asia. *Molecular Ecology*, **24**(11): 2838−2855.
Gwitira I, Murwira A, Shekede MD, Masocha M, Chapano C. 2014. Precipitation of the warmest quarter and temperature of the warmest month are key to understanding the effect of climate change on plant species diversity in Southern African savannah. *African Journal of Ecology*, **52**(2): 209−216.
Hijmans RJ, Cameron SE, Parra JL, Jones PG, Jarvis A. 2005. Very high resolution interpolated climate surfaces for global land areas. *International Journal of Climatology*, **25**(15): 1965−1978.
Jackson DA. 1993. Stopping rules in principal components analysis: a comparison of heuristical and statistical approaches. *Ecology*, **74**(8): 2204−2214.
Jacobs DS, Babiker H, Bastian A, Kearney T, Van Eeden R, Bishop JM. 2013. Phenotypic convergence in genetically distinct lineages of a *Rhinolophus* species complex (Mammalia, Chiroptera). *PLoS One*, **8**(12): e82614.
Jacobs DS, Bastian A. 2018. High duty cycle echolocation may constrain the evolution of diversity within horseshoe bats (Family: Rhinolophidae). *Diversity*, **10**(3): 85.
Jones G. 1999. Scaling of echolocation call parameters in bats. *Journal of Experimental Biology*, **202**(23): 3359−3367.
Jones G, Holderied MW. 2007. Bat echolocation calls: adaptation and convergent evolution. *Proceedings of the Royal Society B:Biological Sciences*, **274**(1612): 905−912.
Jones G, Teeling EC. 2006. The evolution of echolocation in bats. *Trends in Ecology & Evolution*, **21**(3): 149−156.
Kembel SW, Cowan PD, Helmus MR, Cornwell WK, Morlon H, Ackerly DD, et al. 2010. Picante: R tools for integrating phylogenies and ecology. *Bioinformatics*, **26**(11): 1463−1464.
Lanfear R, Calcott B, Ho SYW, Guindon S. 2012. PartitionFinder: combined selection of partitioning schemes and substitution models for phylogenetic analyses. *Molecular Biology and Evolution*, **29**(6): 1695−1701.
Losos JB. 2008. Phylogenetic niche conservatism, phylogenetic signal and the relationship between phylogenetic relatedness and ecological similarity among species. *Ecology Letters*, **11**(10): 995−1003.
Machac A, Storch D, Wiens JJ. 2013. Ecological causes of decelerating diversification in carnivoran mammals. *Evolution*, **67**(8): 2423−2433.
Maluleke T, Jacobs DS, Winker H. 2017. Environmental correlates of geographic divergence in a phenotypic trait: a case study using bat echolocation. *Ecology and Evolution*, **7**(18): 7347−7361.
Mazel F, Davies TJ, Gallien L, Renaud J, Groussin M, Münkemüller T, et al. 2016. Influence of tree shape and evolutionary time‐scale on phylogenetic diversity metrics. *Ecography*, **39**(10): 913−920.
McKenna MC, Bell SK. 1997. Classification of mammals above the species level. New York: Columbia University Press.
Meredith RW, Janečka JE, Gatesy J, Ryder OA, Fisher CA, Teeling EC, et al. 2011. Impacts of the Cretaceous Terrestrial Revolution and KPg extinction on mammal diversification. *Science*, **334**(6055): 521−524.
Moen D, Morlon H. 2014. Why does diversification slow down?. *Trends in Ecology & Evolution*, **29**(4): 190−197.
Morley RJ. 2003. Interplate dispersal paths for megathermal angiosperms. *Perspectives in Plant Ecology, Evolution and Systematics*, **6**(1–2): 5–20.
Morlon H, Lewitus E, Condamine FL, Manceau M, Clavel J, Drury J. 2016. RPANDA: an R package for macroevolutionary analyses on phylogenetic trees. *Methods in Ecology and Evolution*, **7**(5): 589−597.
Morlon H, Parsons TL, Plotkin JB. 2011. Reconciling molecular phylogenies

with the fossil record. *Proceedings of the National Academy of Sciences of the United States of America*, **108**(39): 16327−16332.

Mutumi GL, Jacobs DS, Winker H. 2017. The relative contribution of drift and selection to phenotypic divergence: a test case using the horseshoe bats *Rhinolophus simulator* and *Rhinolophus swinnyi*. *Ecology and Evolution*, **7**(12): 4299–4311.

Paradis E, Claude J, Strimmer K. 2004. APE: analyses of phylogenetics and evolution in R language. *Bioinformatics*, **20**(2): 289−290.

Pfennig K, Pfennig D. 2009. Character displacement: ecological and reproductive responses to a common evolutionary problem. *The Quarterly Review of Biology*, **84**(3): 253−276.

R Core Team. 2018. R: a language and environment for statistical computing. Vienna: R Foundation for Statistical Computing.

Rabosky DL. 2013. Diversity-dependence, ecological speciation, and the role of competition in macroevolution. *Annual Review of Ecology, Evolution, and Systematics*, **44**: 481−502.

Rabosky DL, Donnellan SC, Grundler M, Lovette IJ. 2014a. Analysis and visualization of complex macroevolutionary dynamics: an example from Australian scincid lizards. *Systematic Biology*, **63**(4): 610−627.

Rabosky DL, Grundler M, Anderson C, Title P, Shi JJ, Brown JW, et al. 2014b. BAMMtools: an R package for the analysis of evolutionary dynamics on phylogenetic trees. *Methods in Ecology and Evolution*, **5**(7): 701−707.

Ravel A, Marivaux L, Qi T, Wang YQ, Beard KC. 2014. New chiropterans from the middle Eocene of Shanghuang (Jiangsu Province, Coastal China): new insight into the dawn horseshoe bats (Rhinolophidae) in Asia. *Zoologica Scripta*, **43**(1): 1−23.

Rebelo H, Tarroso P, Jones G. 2010. Predicted impact of climate change on European bats in relation to their biogeographic patterns. *Global Change Biology*, **16**(2): 561−576.

Scotese CR. 2001. Atlas of earth history. PALEOMAP project. Arlington (TX),http://www.scotese.com.

Shi JJ, Rabosky DL. 2015. Speciation dynamics during the global radiation of extant bats. *Evolution*, **69**(6): 1528−1545.

Simmons NB. 2005. Order chiroptera. *In*: Wilson DE, Reeder DM. Mammal Species of the World: A Taxonomic and Geographic Reference. 3rd ed. Baltimore: The Johns Hopkins University Press.

Simmons NB, Geisler JH. 1998. Phylogenetic relationships of Icaronycteris, Archaeonycteris, Hassianycteris, and Palaeochiropteryx to extant bat lineages, with comments on the evolution of echolocation and foraging strategies in Microchiroptera. *Bulletin of the American Museum of Natural History*, **235**: 188−192.

Stamatakis A. 2014. RAxML version 8: a tool for phylogenetic analysis and post-analysis of large phylogenies. *Bioinformatics*, **30**(9): 1312−1313.

Steeman ME, Hebsgaard MB, Fordyce RE, Ho SYW, Rabosky DL, Nielsen R, et al. 2009. Radiation of extant Cetaceans driven by restructuring of the oceans. *Systematic Biology*, **58**(6): 573−585.

Stoffberg S, Jacobs DS, Mackie IJ, Matthee CA. 2010. Molecular phylogenetics and historical biogeography of *Rhinolophus* bats. *Molecular Phylogenetics and Evolution*, **54**(1): 1−9.

Stoffberg S, Jacobs DS, Matthee CA. 2011. The divergence of echolocation frequency in horseshoe bats: moth hearing, body size or habitat?. *Journal of Mammalian Evolution*, **18**(2): 117−129.

Suchard MA, Lemey P, Baele G, Ayres DL, Drummond AJ, Rambaut A. 2018. Bayesian phylogenetic and phylodynamic data integration using BEAST 1.10. *Virus Evolution*, **4**(1): vey016.

Sun KP, Luo L, Kimball RT, Wei XW, Jin LR, Jiang TL, et al. 2013. Geographic variation in the acoustic traits of greater horseshoe bats: testing the importance of drift and ecological selection in evolutionary processes. *PLoS One*, **8**(8): e70368.

Swartz SM, Freeman PW, Stockwell EF. 2003. Ecomorphology of bats: comparative and experimental approaches relating structural design to ecology. *In*: Kunz TH, Fenton MB. Bat Ecology. Chicago: The University of Chicago Press, 257–300.

Taylor PJ, Stoffberg S, Monadjem A, Schoeman MC, Bayliss J, Cotterill FPD. 2012. Four new bat species (*Rhinolophus hildebrandtii* complex) reflect plio-pleistocene divergence of dwarfs and giants across an Afromontane archipelago. *PLoS One*, **7**(9): e41744.

Teeling EC, Springer MS, Madsen O, Bates P, O'brien SJ, Murphy WJ. 2005. A molecular phylogeny for bats illuminates biogeography and the fossil record. *Science*, **307**(5709): 580−584.

Thomas JA, Moss CF, Vater M. 2004. Echolocation in Bats and Dolphins. Chicago: University of Chicago Press.

Voje KL, Holen ØH, Liow LH, Stenseth NC. 2015. The role of biotic forces in driving macroevolution: beyond the Red Queen. *Proceedings of the Royal Society B:Biological Sciences*, **282**(1808): 20150186.

Weir JT, Mursleen S. 2013. Diversity‐dependent cladogenesis and trait evolution in the adaptive radiation of the auks (Aves: Alcidae). *Evolution:International Journal of Organic Evolution*, **67**(2): 403−416.

Wiens JJ. 2011. The causes of species richness patterns across space, time, and clades and the role of “ecological limits”. *The Quarterly Review of Biology*, **86**(2): 75−96.

Willig MR. 2003. Patterns of range size, richness, and body size in the Chiroptera. *In*: Kunz TH, Fenton MB. Bat Ecology. Chicago: The University of Chicago Press, 580–621.

Wilson DE, Mittermeier RA. 2019. Handbook of the Mammals of the World: Vol. 9 Bats. Barcelona: Lynx.

Yoder JB, Clancey E, Des Roches S, Eastman JM, Gentry L, Godsoe W, et al. 2010. Ecological opportunity and the origin of adaptive radiations. *Journal of Evolutionary Biology*, **23**(8): 1581−1596.

Yu W, Wu Y, Yang G. 2014. Early diversification trend and Asian origin for extent bat lineages. *Journal of Evolutionary Biology*, **27**(10): 2204−2218.

Yu WH, Xu JX, Wu Y, Yang G. 2012. A comparative study of mammalian diversification pattern. *International Journal of Biological Sciences*, **8**(4): 486−497.

Yu Y, Harris AJ, Blair C, He XJ. 2015. RASP (Reconstruct Ancestral State in Phylogenies): a tool for historical biogeography. *Molecular Phylogenetics and Evolution*, **87**: 46−49.